A Hammerstein Diversity Combining Technique

Amir Masoud Aminian-Modarres
Department of Electrical Engineering
Ferdowsi University of Mashhad
Mashhad, Iran
aminian.mod@gmail.com

Mohammad Molavi-kakhki
Department of Electrical Engineering
Ferdowsi University of Mashhad
Mashhad, Iran
molavi@um.ac.ir

Abstract— In wireless communication channels fading phenomenon imposes serious limitations upon the system performance. Diversity combining is a well known fading compensation technique. In this paper we propose a diversity combining technique based on a nonlinear Hammerstein type filter to mitigate the destructive fading effect. In the present work, frequency selective Rayleigh fading channels in presence of additive white gaussian noise are considered and m-ary PAM modulation is employed. We first present a theoretical analysis to justify our proposed system. Then the system performance for different power delay profiles and different m-ary PAM modulations are investigated. Comparison of simulation results based on our proposed technique with the results obtained when linear equalizing filters are employed, shows that our technique leads to a considerably higher BER performance at higher SNRs. We also show that our method has a lower complexity than the linear structure. Also, a relative reliability factor for the system is defined and investigated.

Keywords- nonlinear diversity combining, Hammerstein filter, nonlinear equalizer, frequency selective fading channel

I. INTRODUCTION

Wireless communication systems suffer from the destructive effects of channel fading on the received signal. Diversity combining is a well known technique for combating the effects of fading phenomenon. Space, frequency, time and coding diversities, and also the combination of two or more of these, have been used in different systems. Various techniques have been suggested for combining the multiple received signals [1]-[6]. In presence of additive white gaussian noise, maximal ratio combining (MRC), which is a linear technique, is the optimum diversity receiver for flat fading channels [2].

In frequency selective channels, the received signal is perturbed by intersymbol interference (ISI) as well as noise. In this case the optimum receiver employs maximum likelihood sequence estimation (MLSE) method [1]. However, MLSE is a nonlinear method with a high computational complexity that increases exponentially with the channel memory length.

There are also suboptimum receivers that employ various types of equalization methods for compensating the ISI effect. Linear equalizer and decision feedback equalizer (DFE) are the most usual methods for equalization [1]. Linear equalizer utilizes a simple linear transversal filter and therefore has a very low complexity. Also in DFE, linear transversal filters are employed as feedforward and feedback blocks. Furthermore, in single-input multiple-output (SIMO) frequency selective channels, linear and decision feedback equalizers can be employed in each diversity branch [1].

In this work we offer a low complexity, nonlinear diversity combining technique for SIMO frequency

selective Rayleigh fading channels, which is based on Hammerstein type filters. Hammerstein filter is a nonlinear polynomial filter used in many applications such as system identification [7]-[9], modeling [10], [11], echo cancelation [12], [13], and noise cancelation [14]. Hammerstein decision feedback equalization (HDFE) has been employed in fiber-wireless channel to compensate for nonlinear distortion in the electrical-to-optical converter [15], [16]. HDFE has also been proposed for GSM receivers as an alternative to the existing methods [17]. Moreover blind HDFE has been proposed in order to enhance the spectral efficiency of the system [18]. In these works, single-input single-output (SISO) model is assumed for their communication systems and the fading effect is not discussed.

This paper is organized as follows. In section 2 we present the system model. Section 3 introduces our nonlinear Hammerstein diversity combining technique. Theoretical analysis of our proposed system is presented in section 4. Section 5, provides the simulation results followed by a discussion. The complexities of nonlinear and linear techniques are compared in section 6, before concluding the paper in section 7.

II. SYSTEM MODEL

The equivalent low-pass discrete time model of the system is illustrated in Fig. 1. In this work we employ m-ary PAM modulation, and the transmitted sequence $x(n)$ is drawn from an i.i.d. source with equi-probable symbols. The symbol amplitudes, A_i, take the discrete levels:

$$A_i = (2i - 1 - m)d \qquad i = 1, 2, ..., m \qquad (1)$$

where m is the number of possible symbols and $2d$ is the distance between adjacent symbol amplitudes.

The SIMO channel consists of M diversity branches. Each branch is assumed to be a frequency selective Rayleigh fading channel, modeled by a tapped delay line with L taps. Hence the channel tap gains can be presented by an $M \times L$ matrix as:

$$\mathbf{H} = \begin{bmatrix} h_{11} & h_{12} & \cdots & h_{1L} \\ h_{21} & h_{22} & \cdots & h_{2L} \\ \vdots & & & \\ h_{M1} & h_{M2} & \cdots & h_{ML} \end{bmatrix} \qquad (2)$$

where h_{ij} is the complex Rayleigh distributed random gain of the jth tap of the ith channel:

$$h_{ij} = h_{Iij} + j h_{Qij} \qquad (3)$$

h_{Iij} and h_{Qij} are the real and the imaginary component of the channel gain respectively. These two components are independent, zero mean, gaussian random variables with variance σ_{hij}^2. Furthermore, the tap gains are assumed uncorrelated and normalized to unity, i.e. :

$$E\{h_{ij} h_{kl}^*\} = 0 \qquad for \ i \neq k \ or \ j \neq l \qquad (4)$$

and:

$$\sum_{j=1}^{L} E\{|h_{ij}|^2\} = 1 \qquad for \quad i = 1, 2, ..., M \qquad (5)$$

In this work the channel fading is assumed sufficiently slow, such that the tap gains do not vary during one data frame. We also assume that all of the M frequency selective channels have identical power delay profiles (PDP). PDP is the profile of the mean square values of the tap gains. Examples of these profiles used in our simulations are presented in section 5.

The received signal from the ith channel which is corrupted by ISI and noise is given by:

$$y_i(n) = \sum_{j=1}^{L} h_{ij} x(n - j + 1) + w_i(n) \qquad i = 1, 2, ..., M \qquad (6)$$

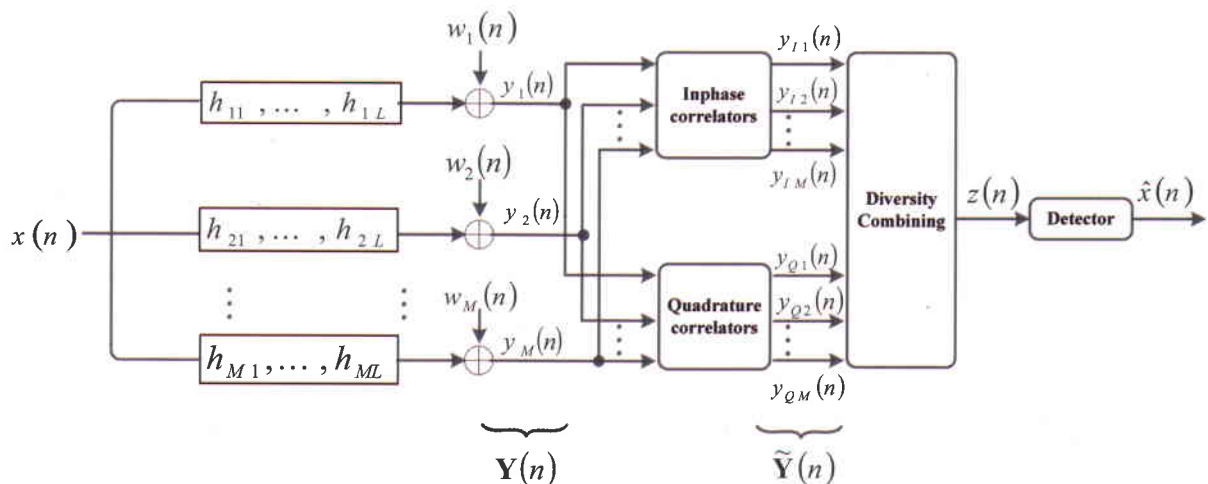where $w_i(n)$ is the complex additive white gaussian noise at the ith receiver branch:

Fig. 1. System model

$$w_i(n) = w_{Ii}(n) + j\, w_{Qi}(n) \qquad (7)$$

$w_{Ii}(n)$ and $w_{Qi}(n)$ are uncorrelated, zero mean, gaussian random variables with variance σ_w^2. Equation (6) can be expressed in matrix form:

$$\mathbf{Y}(n) = \mathbf{H}\,\mathbf{X}(n) + \mathbf{W}(n) \qquad (8)$$

where $\mathbf{H}$ is the channel matrix and $\mathbf{Y}(n)$, $\mathbf{X}(n)$ and $\mathbf{W}(n)$ are the received data vector, the transmitted data vector and the noise vector respectively. These vectors are defined as follows:

$$\mathbf{Y}(n) = \left[\, y_1(n) \ldots y_M(n) \,\right]^{\mathrm{T}} \qquad (9)$$

$$\mathbf{X}(n) = \left[\, x(n) \quad x(n-1) \ldots x(n-L+1) \,\right]^{\mathrm{T}} \qquad (10)$$

$$\mathbf{W}(n) = \left[\, w_1(n) \ldots w_M(n) \,\right]^{\mathrm{T}} \qquad (11)$$

As shown in Fig. 1, the receiver consists of two correlators banks, namely, inphase and quadrature correlators. The complex received signal $y_i(n)$ from each branch is applied to both correlators. The outputs of the inphase and quadrature correlators are the real part $\left(y_{Ii}(n) \right)$ and the imaginary part $\left(y_{Qi}(n) \right)$ of $y_i(n)$ respectively. According to equations (3) and (7), we can write:

$$y_{Ii}(n) = \sum_{j=1}^{L} h_{Iij}\, x(n-j+1) + w_{Ii}(n) \qquad i=1,2,\ldots,M$$
$$y_{Qi}(n) = \sum_{j=1}^{L} h_{Qij}\, x(n-j+1) + w_{Qi}(n) \qquad (12)$$

We define the $2M \times 1$ real vector $\widetilde{\mathbf{Y}}(n)$ as:

$$\begin{aligned}
\widetilde{\mathbf{Y}}(n) &= \left[\, \widetilde{y}_1(n) \quad \widetilde{y}_2(n) \ \ldots \ \widetilde{y}_{2M}(n) \,\right]^{\mathrm{T}} \\
&= \left[\, y_{I1}(n) \ \ldots \ y_{IM}(n) \ y_{Q1}(n) \ldots \ y_{QM}(n) \,\right]^{\mathrm{T}}
\end{aligned} \qquad (13)$$

where:

$$\widetilde{y}_i(n) = \begin{cases} y_{Ii}(n) & 1 \le i \le M \\ y_{Q(i-M)}(n) & M+1 \le i \le 2M \end{cases} \qquad (14)$$

This model is very convenient for computational purposes, as we deal with real values only. It is in fact similar to having $2M$ real diversity branches. As shown in Fig. 1, $\widetilde{\mathbf{Y}}(n)$ is the input to the diversity combining filters. Then, the output of the combiner, $z(n)$, is applied to a hard detector for making the output decision $\hat{x}(n)$.

III. NONLINEAR HAMMERSTEIN COMBINING TECHNIQUE

Hammerstein Diversity Combining (HDC) system is shown in Fig. 2. In this approach a Hammerstein filter of order D, is employed for each diversity branch. The output polynomial of the ith filter is:

$$z_i(n) = \sum_{k=1(k\,odd)}^{D} g_{ik}\, \widetilde{y}_i^{\,k}(n) \qquad i=1,2,\ldots,2M \qquad (15)$$

where g_{ik} is the kth coefficient of the output polynomial of the ith filter, and $\widetilde{y}_i(n)$ is defined by equation (14). Note that since our system is memoryless, no delay term appears in equation (15). Also note that only odd powers exist in the summation of equation (15). We will prove in the next section that the terms corresponding to the even powers are equal to zero.

The filters outputs are summed to produce the combiner output $z(n)$, i.e. :

$$z(n) = \sum_{i=1}^{2M} \sum_{k=1(k\,odd)}^{D} g_{ik}\, \widetilde{y}_i^{\,k}(n) \qquad (16)$$

Equation (16) can be expressed in matrix form:

$$z(n) = \mathbf{G}_{\mathbf{H}}^{\mathrm{T}}\, \mathbf{Y}_{\mathbf{H}}(n) \qquad (17)$$

where $\mathbf{G}_{\mathbf{H}}$ is a $M(D+1) \times 1$ vector that consists of coefficients g_{ik}, and $\mathbf{Y}_{\mathbf{H}}(n)$ is a $M(D+1) \times 1$ vector defined as:

$$\mathbf{Y}_{\mathbf{H}}(n) = \left[\, \mathbf{Y}_1^{\mathrm{T}}(n) \quad \widetilde{\mathbf{Y}}_3^{\mathrm{T}}(n) \quad \widetilde{\mathbf{Y}}_5^{\mathrm{T}}(n) \quad \ldots \quad \mathbf{Y}_{\mathbf{D}}^{\mathrm{T}}(n) \,\right]^{\mathrm{T}}, \ D\ odd \qquad (18)$$

where $\widetilde{\mathbf{Y}}_{\mathbf{p}}(n)$ is defined as the pth power of $\widetilde{\mathbf{Y}}(n)$:
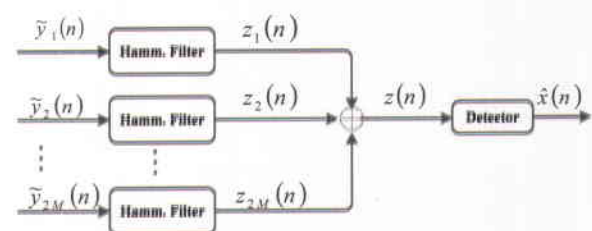
Fig. 2. Hammerstein Diversity Combining Technique (HDC)

$$\widetilde{\mathbf{Y}}_\mathbf{p}(n)=\begin{bmatrix}\widetilde{y}_1^p(n) & \widetilde{y}_2^p(n) & \dots & \widetilde{y}_{2M}^p(n)\end{bmatrix}^\mathsf{T} \quad (19)$$

$z(n)$ is an estimate of the transmitted symbol $x(n)$. Our goal is to find the coefficients g_{ik} such that the mean square error is minimized.

The coefficients of the Hammerstein filters are found from the training mode by using the MSE criterion. In this mode, the transmitter sends a training sequence that is assumed to be known to the receiver as the desired signal $d(n)$. The error signal is defined as difference between the desired and estimated values:

$$e(n)=d(n)-z(n)=x(n)-z(n) \quad (20)$$

The cost function is defined as below:

$$\zeta = E\left\{e^2(n)\right\} \quad (21)$$

where $E\{.\}$ denotes the statistical expectation. Then, the coefficients of HDC system can be computed such that to minimize ζ:

$$\mathbf{G_H}_{opt} = \mathbf{R_H}^{-1}\mathbf{P_H} \quad (22)$$

where $\mathbf{P_H}$ is the $M(D+1)\times 1$ crosscorrelation vector:

$$\mathbf{P_H} = E\left\{\mathbf{Y_H}(n)x(n)\right\} \quad (23)$$

and $\mathbf{R_H}$ is the $M(D+1)\times M(D+1)$ autocorrelation matrix:

$$\mathbf{R_H} = E\left\{\mathbf{Y_H}(n)\mathbf{Y_H}^\mathsf{T}(n)\right\} \quad (24)$$

Since we would like to compare our system with the linear structure, a brief review of linear combining technique is presented here. Linear Diversity Combining system (LDC) is shown in Fig. 3. In this technique, a linear transversal filter with L_{eq} taps is employed for each diversity branch. These filters are designed based on the minimum mean square error (MSE) criterion. The output $z_i(n)$ of the ith filter is:

$$z_i(n)=\sum_{k=-(L_{eq}-1)/2}^{(L_{eq}-1)/2}\hat{g}_{ik}\,\widetilde{y}_i(n-k) \qquad i=1,2,\dots,2M \quad (25)$$

where $\hat{g}_{ik}$ is the kth coefficient of the ith filter. The output of the linear combiner can then be written as:

$$z(n)=\sum_{i=1}^{2M}\sum_{k=-(L_{eq}-1)/2}^{(L_{eq}-1)/2}\hat{g}_{ik}\,\widetilde{y}_i(n-k) \quad (26)$$

Equation (26) can be expressed in matrix form:

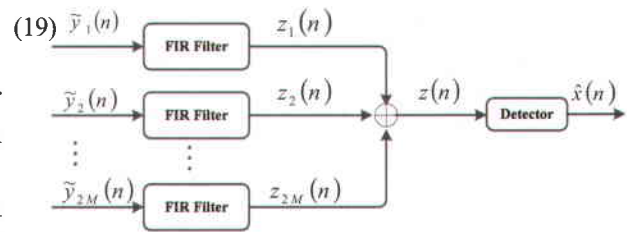$$z(n)=\mathbf{G_L}^\mathsf{T}\mathbf{Y_L}(n) \quad (27)$$

Fig. 3. Linear Diversity Combining Technique (LDC)

where $\mathbf{G_L}$ is a $2ML_{eq}\times 1$ vector that consists of coefficients $\hat{g}_{ik}$, and $\mathbf{Y_L}(n)$ is a $2ML_{eq}\times 1$ vector defined as:

$$\mathbf{Y_L}(n)=\left[\widetilde{\mathbf{Y}}^\mathsf{T}\left(n+\frac{L_{eq}-1}{2}\right) \dots \widetilde{\mathbf{Y}}^\mathsf{T}(n) \dots \widetilde{\mathbf{Y}}^\mathsf{T}\left(n-\frac{L_{eq}-1}{2}\right)\right]^\mathsf{T} \quad (28)$$

where $\widetilde{\mathbf{Y}}(n)$ is defined in equation (13). We can obtain the coefficients of LDC by using the MSE criterion:

$$\mathbf{G_L}_{opt} = \mathbf{R_L}^{-1}\mathbf{P_L} \quad (29)$$

where $\mathbf{P_L}$ is the crosscorrelation vector:

$$\mathbf{P_L} = E\left\{\mathbf{Y_L}(n)x(n)\right\} \quad (30)$$

and $\mathbf{R_L}$ is the autocorrelation matrix:

$$\mathbf{R_L} = E\left\{\mathbf{Y_L}(n)\mathbf{Y_L}^\mathsf{T}(n)\right\} \quad (31)$$

IV. Theoretical Analysis

A. Analysis of the Coefficients

In this subsection we prove that the even coefficients in equation (16) are equal to zero. To do so, we consider the case where $M=2$, $D=3$, and the channel length $L=2$, and assume real channel and noise for simplicity. However, these assumptions do not change the generality and our proof is valid for all cases.
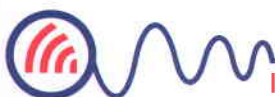
In this case the two received signals are:

$$\begin{aligned}y_1(n) &= h_{11}x(n)+h_{12}x(n-1)+w_1(n)\\ y_2(n) &= h_{21}x(n)+h_{22}x(n-1)+w_2(n)\end{aligned} \quad (32)$$

Also, from our basic assumptions in this work, we have:

$$E\left\{x^k(n)\right\}=\begin{cases}0 & \text{if } k \text{ is odd}\\ n.z.v. & \text{if } k \text{ is even}\end{cases} \quad (33)$$

and:

$$E\left\{w_i^k(n)\right\}=\begin{cases}0 & \text{if } k \text{ is odd}\\ n.z.v. & \text{if } k \text{ is even}\end{cases} \quad (34)$$

where $n.z.v.$ is a none-zero value. From equations (32)-(34), it is easy to show that:

$$E\left\{y_i^k(n)\,y_j^l(n)\right\}=\begin{cases}0 & \text{if } (k+l) \text{ is odd}\\ n.z.v. & \text{if } (k+l) \text{ is even}\end{cases} \quad (35)$$

and:

$$E\left\{y_i^k(n)\,x(n)\right\}=\begin{cases}0 & \text{if } k \text{ is even}\\ n.z.v. & \text{if } k \text{ is odd}\end{cases} \quad (36)$$

For real values of channel and noise we have: $\tilde{y}_1(n)=y_1(n)$, and $\tilde{y}_2(n)=y_2(n)$. Hence, equation (18) becomes:

$$\mathbf{Y_H}(n)=$$
$$\begin{bmatrix} y_1(n) & y_2(n) & y_1^2(n) & y_2^2(n) & y_1^3(n) & y_2^3(n)\end{bmatrix}^\mathbf{T} \quad (37)$$

Substituting equations (35) and (37) in (24), the following form for the autocorrelation matrix is obtained:

$$\mathbf{R_H}=\begin{bmatrix} n.z.v. & n.z.v. & 0 & 0 & n.z.v. & n.z.v.\\ n.z.v. & n.z.v. & 0 & 0 & n.z.v. & n.z.v.\\ 0 & 0 & n.z.v. & n.z.v. & 0 & 0\\ 0 & 0 & n.z.v. & n.z.v. & 0 & 0\\ n.z.v. & n.z.v. & 0 & 0 & n.z.v. & n.z.v.\\ n.z.v. & n.z.v. & 0 & 0 & n.z.v. & n.z.v.\end{bmatrix} \quad (38)$$

where the blocks of the matrix are alternatively zero and none-zero. It is easy to show that the inverse matrix $\mathbf{R_H^{-1}}$ has also a similar form.

On the other hand, substituting equations (36) and (37) in (23), the following form for the crosscorrelation vector is obtained:

$$\mathbf{P_H}=\begin{bmatrix} n.z.v. & n.z.v. & 0 & 0 & n.z.v. & n.z.v.\end{bmatrix}^\mathbf{T} \quad (39)$$

If we substitute $\mathbf{R_H^{-1}}$ and $\mathbf{P_H}$ in equation (22), we have:

$$\mathbf{G_H}_{opt}=\begin{bmatrix} n.z.v. & n.z.v. & 0 & 0 & n.z.v. & n.z.v.\end{bmatrix}^\mathbf{T} \quad (40)$$

Hence, the even coefficients of the filter are zero. This proof can be easily generalized for arbitrary values of M, D and L.

B. Average Minimum MSE

In this subsection we evaluate the average minimum mean square error (MMSE) for a HDC system, for frequency selective Rayleigh fading channels. Using equations (21), (20) and (17), the MSE value for HDC system can be expressed as:

$$\zeta=E\left\{\left[x(n)-\mathbf{G_H^T}\mathbf{Y_H}(n)\right]\left[x(n)-\mathbf{Y_H^T}(n)\mathbf{G_H}\right]\right\}$$
$$=E\left\{x^2(n)\right\}-2\mathbf{G_H^T}\mathbf{P_H}+\mathbf{G_H^T}\mathbf{R_H}\mathbf{G_H} \quad (41)$$

For a particular channel occurrence, the optimum coefficients of the Hammerstein filters are obtained from equation (22). Replacing $\mathbf{G_H}$ by $\mathbf{G_H}_{opt}$ in equation (41), we have:

$$\zeta_{min}=E\left\{x^2(n)\right\}-\mathbf{P_H^T}\mathbf{R_H^{-1}}\mathbf{P_H} \quad (42)$$

This is the minimum MSE that can be achieved by a HDC system for a particular channel occurrence.

Next, we would like to evaluate the average MMSE, averaged over all possible channel realizations. We first consider the case where $M=2$, $D=3$, and the channel length $L=2$, and assume real channel and noise and also 2-PAM modulation. In this case the two received signals are:

$$y_1(n)=h_{11}x(n)+h_{12}x(n-1)+w_1(n)$$
$$y_2(n)=h_{21}x(n)+h_{22}x(n-1)+w_2(n) \quad (43)$$

Using equations (43), (18), (23) and (24), the 4×1 crosscorrelation and 4×4 autocorrelation matrixes are computed as:

$$\begin{cases}\mathbf{P_H}(1,1)=E\left\{x(n)y_1(n)\right\}=h_{11}\\ \mathbf{P_H}(2,1)=E\left\{x(n)y_2(n)\right\}=h_{21}\\ \mathbf{P_H}(3,1)=E\left\{x(n)y_1^3(n)\right\}=h_{11}^3+3h_{11}h_{12}^2+3h_{11}\sigma_w^2\\ \mathbf{P_H}(4,1)=E\left\{x(n)y_2^3(n)\right\}=h_{21}^3+3h_{21}h_{22}^2+3h_{21}\sigma_w^2\end{cases} \quad (44)$$

and:

$$\begin{cases}\mathbf{R_H}(1,1)=E\left\{y_1(n)y_1(n)\right\}=h_{11}^2+h_{12}^2+\sigma_w^2\\ \mathbf{R_H}(1,2)=E\left\{y_1(n)y_2(n)\right\}=h_{11}h_{21}+h_{12}h_{22}\\ \mathbf{R_H}(1,3)=E\left\{y_1(n)y_1^3(n)\right\}=\dots\\ \mathbf{R_H}(1,4)=E\left\{y_1(n)y_2^3(n)\right\}=\dots\\ \vdots\end{cases} \quad (45)$$

Substituting these matrixes in equation (42), the MMSE can be obtained as a function of particular channel tap gains and the noise variance σ_w^2:

$$\zeta_{min}\left(h_{11},h_{12},h_{21},h_{22},\sigma_w^2\right)=\frac{Num\left(h_{11},h_{12},h_{21},h_{22},\sigma_w^2\right)}{Den\left(h_{11},h_{12},h_{21},h_{22},\sigma_w^2\right)} \quad (46)$$

where:

$$Num=\sigma_w^2[\ (12\,h_{11}\,h_{22})^2\,(h_{11}^2\,h_{22}^4+h_{12}^4\,h_{21}^2)$$
$$+(36\,h_{11}\,h_{12}\,h_{21}\,h_{22})^2\,(h_{12}^2+h_{22}^2)\,] \quad (47)$$

and:

$$Den=16\,(h_{11}^6\,h_{22}^6+h_{21}^6\,h_{12}^6)+(12h_{11}h_{12}h_{21}h_{22})^2(9h_{11}^2\,h_{22}^2$$
$$+9h_{12}^2\,h_{21}^2-2h_{11}^2\,h_{12}^2-2h_{22}^2\,h_{21}^2)-3200\,(h_{11}h_{12}h_{21}h_{22})^3+$$
$$144\,[\ (h_{11}h_{22})^2\,(h_{12}^2\,h_{11}^2h_{22}^4+h_{11}^4\,h_{22}^2h_{21}^2+h_{21}^2\,h_{11}^4h_{12}^2+$$
$$h_{12}^2\,h_{22}^4h_{21}^2+h_{21}^2\,h_{12}^6+h_{21}^6\,h_{12}^2)\ +\ (h_{11}h_{21})^4\,(h_{21}^2\,h_{11}^2+$$
$$h_{22}^2\,h_{12}^2)\ ]+3\sigma_w^2\,(18h_{11}h_{12}h_{21}h_{22})^2(h_{11}^2+h_{12}^2+h_{21}^2+h_{22}^2)+$$
$$1200\,\sigma_w^2(h_{11}h_{12}h_{21}h_{22})\,[\ (h_{11}h_{22})^2(h_{12}^2+h_{21}^2)+(h_{12}h_{21})^2$$
$$(h_{11}^2+h_{22}^2)\ ]-84\sigma_w^2[\ (h_{11}h_{22})^4(h_{11}^2+h_{22}^2+9h_{21}^2+9h_{12}^2)+$$
$$(h_{12}h_{21})^4\,(h_{12}^2+h_{21}^2+9h_{11}^2+9h_{22}^2)\ ]-36\,\sigma_w^2[\ (h_{12}h_{22})^2$$
$$(h_{12}^6+h_{21}^6+h_{11}^4h_{12}^2+h_{22}^4h_{21}^2-2\,h_{11}^2h_{12}^4-2h_{22}^2h_{21}^4-3h_{12}^4h_{22}^2$$
$$-3\,h_{21}^2h_{11}^4)\ +\ (h_{11}h_{21})^2\,(h_{22}^6+h_{11}^6+h_{11}^2h_{12}^4+h_{22}^2h_{21}^4-$$
$$2\,h_{11}^4h_{12}^2-2\,h_{22}^4h_{21}^2-3\,h_{12}^4h_{22}^2-3\,h_{21}^4h_{11}^2)\ ] \quad (48)$$

Note that in equations (47) and (48) we use this approximation:

$$\left(\sigma_w^2\right)^K \approx 0 \qquad for \quad k>1 \tag{49}$$

Then, equation (46) must be averaged over all possible channel realizations. Based on our basic assumptions in this work and using equations (2)-(4), the joint PDF of the channel tap gains is:

$$p\left(h_{11},h_{12},h_{21},h_{22}\right)=\frac{1}{(2\pi)^2\sqrt{\sigma_{h11}^2\,\sigma_{h12}^2\,\sigma_{h21}^2\,\sigma_{h22}^2}}\times$$
$$\exp\left[-0.5\left(\frac{h_{11}^2}{\sigma_{h11}^2}+\frac{h_{12}^2}{\sigma_{h12}^2}+\frac{h_{21}^2}{\sigma_{h21}^2}+\frac{h_{22}^2}{\sigma_{h22}^2}\right)\right] \tag{50}$$

Finally, the average MMSE is computed as below:

$$\zeta_{min}\left(\sigma_w^2\right)=\int\int\int\int \zeta_{min}\left(h_{11},h_{12},h_{21},h_{22},\sigma_w^2\right)\times$$
$$p\left(h_{11},h_{12},h_{21},h_{22}\right)dh_{11}\,dh_{12}\,dh_{21}\,dh_{22} \tag{51}$$

It is difficult to obtain a close-form for this equation. Therefore, we should compute it by numerical methods.

Generalization of this approach for arbitrary values of M, D, L and m-ary PAM, leads to similar equations. In the next section we will present an example of this numerical solution for evaluating the average MMSE.

V. SIMULATION RESULTS AND DISCUSSIONS

In this section the average error rate is evaluated for HDC and LDC techniques, by the simulation results. Also, the average MMSE for a HDC system is evaluated numerically and is compared with the simulation result. The reliability of HDC technique is discussed, too. The simulations are performed for four different frequency selective Rayleigh channels with power delay profiles shown in Fig. 4. These are the examples of common profiles used in wireless communication channels [2], [20], [21]. We generate 200,000 random realizations of the channel and obtain the average system performance by Monte Carlo simulations. We also use a 100-bit sequence for training mode.

A. Average System Performance

In this subsection the average system performance for HDC and LDC systems using the channel profile (a), is presented.

First, we consider 2-PAM (BPSK) modulation. In Fig. 5, the average bit error rate (BER) versus SNR is shown for HDC and LDC techniques. In these simulations, which are performed for three different number of diversity branches $M\in\{2,3,4\}$, we choose the order of Hammerstein filter $D=5$ and the number of linear filter taps $L_{eq}=5$. From this figure, we observe that at higher SNRs HDC has a considerable better performance than LDC. For example, for $M=4$, when
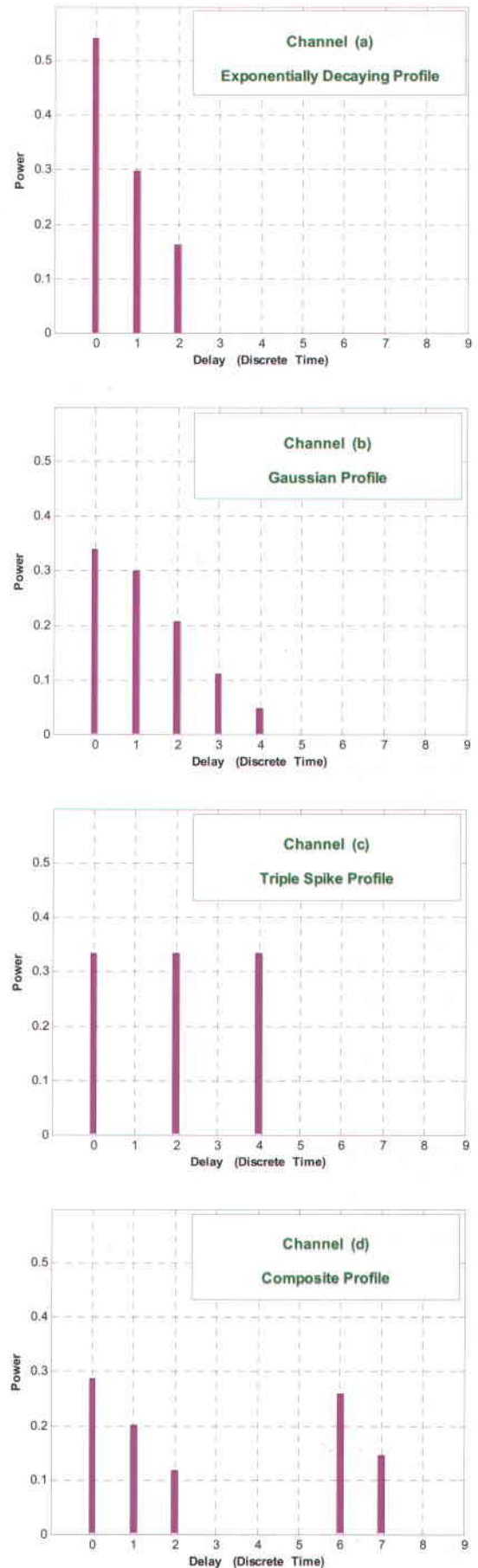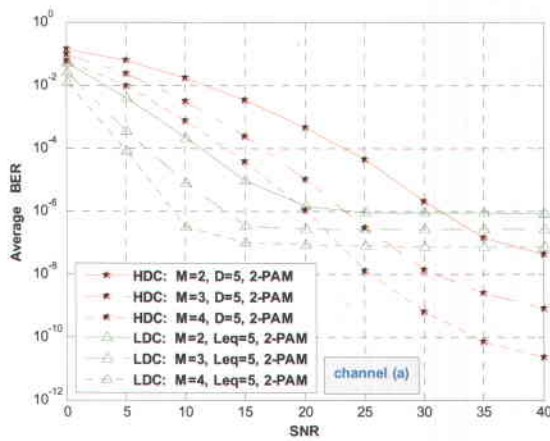

Fig 4. Four examples for channel PDP

Fig. 5. Average BER for the channel (a)

Fig. 7. The effect of increasing polynomial order in HDC

the $SNR = 40\,dB$, the average BER of HDC is almost 10000 times lower than LDC, which is a valuable advantage of our proposed technique. However, the disadvantage of HDC at lower SNRs, is due to the inherent property of all nonlinear systems at low signal to noise ratios. Examples of these behaviors are observed in decision feedback equalizers and FM modulators, in which their superiority over linear techniques appears when SNR is above a threshold.

To prove the validity of the above comparison when the number of taps in LDC is increased, we evaluate the average BER of this technique for different number of taps $L_{eq} \in \{3, 5, 11\}$ and $M = 3$. As can be seen from Fig. 6, the performance dose not change considerably when L_{eq} is increased. Hence, increasing the number of taps in LDC, does not change the superiority of HDC.

To see the effect of the polynomial order D on the performance of HDC, simulations are performed for three different values of $D \in \{3, 5, 7\}$ when $M = 3$. The results of these simulations are presented in Fig. 7. As can be seen from this figure, when $D > 5$, the system performance dose not change notably. Hence, in this work we choose $D = 5$.

Next, the results for different m-ary PAMs are presented. We consider equal average energy for transmitted symbols. Hence, from equation (1), we need
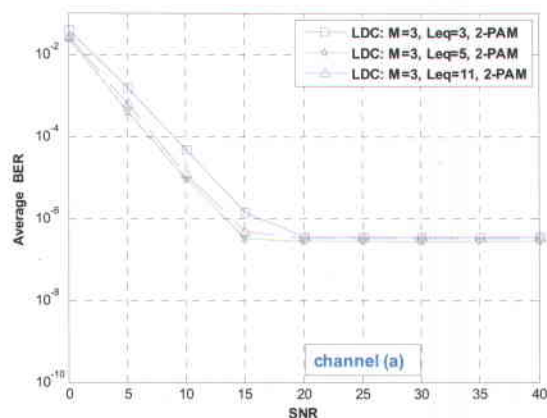
to choose $d = 1$, $d = 1/\sqrt{5}$ and $d = 1/\sqrt{21}$ for $m = 2$, $m = 4$ and $m = 8$, respectively. In other words, as m is increased, the distance between adjacent symbol amplitudes decreases.

Figs. 8 and 9 show the average symbol error rate (SER), for 4-PAM and 8-PAM respectively. The system parameters are taken as $M \in \{3, 4, 5\}$, $D = 5$, and $L_{eq} = 5$ in Fig. 8, and $M \in \{4, 5, 6\}$, $D = 5$, and $L_{eq} = 5$ in Fig. 9. Comparing these figures with Fig. 5, we
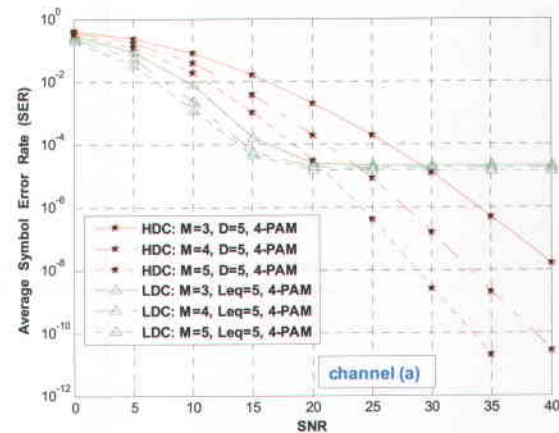

Fig. 8. Average SER for the channel (a)_ 4-PAM modulation

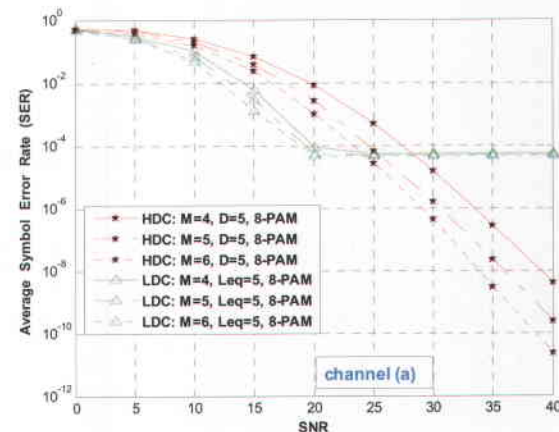Fig. 6. The effect of increasing the number of taps in LDC

Fig. 9. Average SER for the channel (a)_ 8-PAM modulation

observe that the superiority of HDC to LDC is valid for any m. In Fig. 10, the results of our simulations are shown for three different PAMs with $m \in \{2, 4, 8\}$, when $M = 4$, $D = 5$, and $Leq = 5$.

To see another aspect of HDC and LDC techniques, we investigate the effect of the number of diversity branches on the average performance of HDC and LDC techniques, when m-arry PAM modulation is employed. In Fig. 11 we show the average SER of these techniques for three different values of M for $SNR = 35\ dB$. As can be seen from this figure, the system performance of LDC dose not change considerably when M is increased, especially for higher values of m. On the other hand, the system performance of HDC is improved by increasing the number of diversity branches.

In Fig. 12, the average MMSE for a HDC system is evaluated numerically, based on equation (51), and the obtained result is compared with the simulation result. In this case, the channel (a) is employed and the parameters are $M = 2$, $m = 2$ and $D = 5$. From this figure, we observe that the two curves are close together. This means that the approach presented in subsection 4-2, verifies our simulation results.
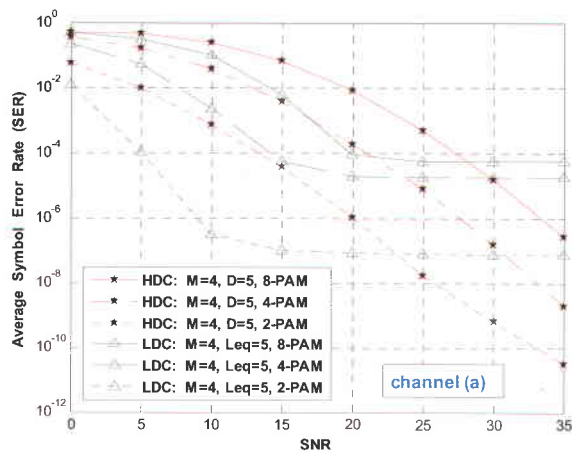

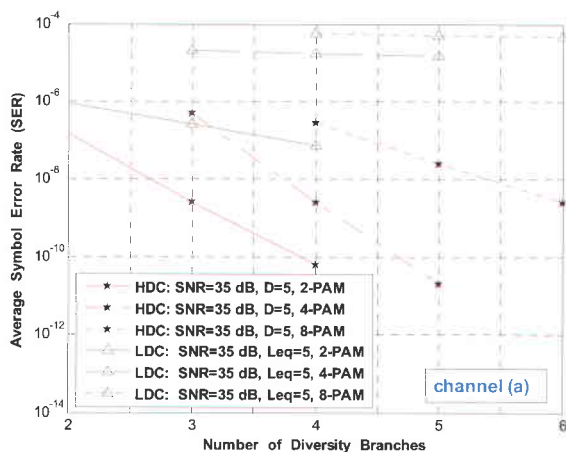Fig. 10. Average SER for three different PAMs

Fig. 11. The effect of the number of diversity branches on the average SER for three different PAMs
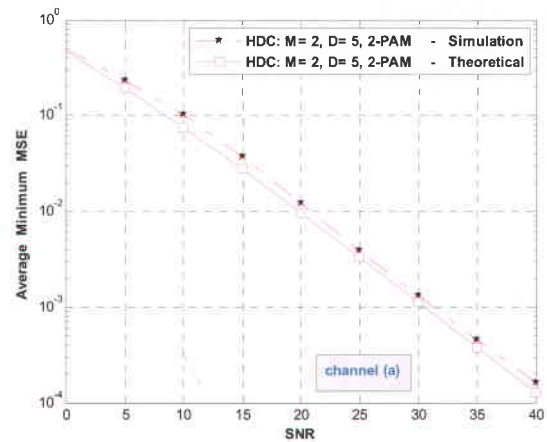

Fig. 12. The average MMSE for HDC system

B. Results for Different PDPs

The power delay profile (PDP) reflects the propagation environment. Here, we investigate the effect of different PDPs on the performance of LDC and HDC techniques.

The channel profiles (a), (b), (c), and (d) in Fig. 4 are the examples of exponentially decaying profiles [2], gaussian profiles [20], triple spike profiles [20], and composite profiles [21], respectively. The system performance for the channel (a) was shown before in Fig. 5. Figs. 13 and 14 show the results of similar simulations for the channel profiles (b) and (c) respectively. In these simulations the system parameters are chosen as $M \in \{4, 5\}$, $m = 2$, $D = 5$, and $L_{eq} = 9$. In Fig. 15, the performances of LDC and HDC techniques are compared for the channel (d). The parameters are taken as $M \in \{4, 5\}$, $m = 2$, $D = 5$, and $Leq = 15$. From Figs. 5, 13, 14 and 15, it is observed that the superiority of HDC to LDC is valid for all different PDPs.

C. Reliability

In the previous subsections, we evaluated the average BER and SER performance; averaged over all possible
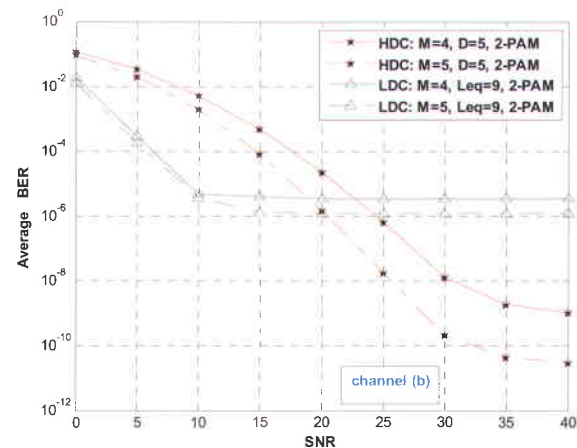

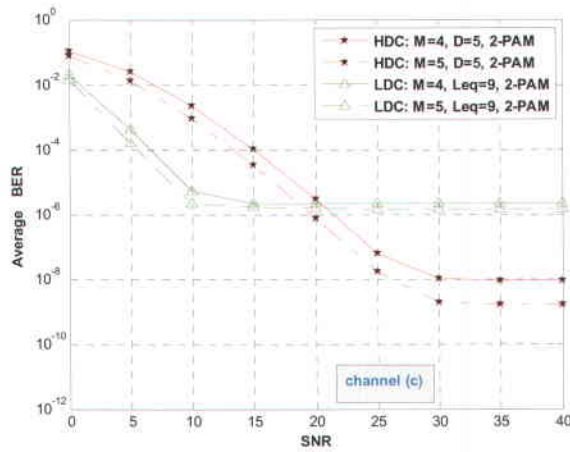Fig. 13. Average BER for the channel (b)
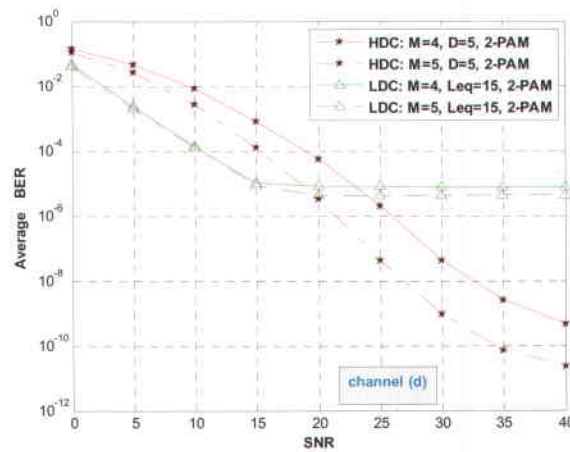
Fig. 14. Average BER for the channel (c)

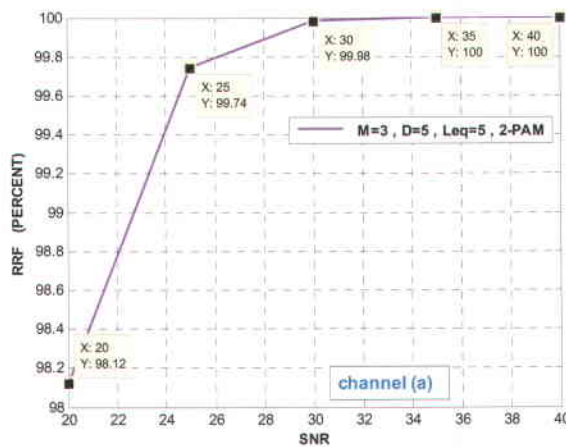Fig. 15. Average BER for the channel (d)

Fig. 16. Relative reliability factor

channel realizations. There are some rare channel realizations that cause significant error rate. These infrequent occurrences reduce the average system performance. However, in many practical situations like voice communications, the important factor for the user is the system performance for any individual channel occurrences rather than the average system performance.

Here we focus on individual channel realizations and compare the performance of HDC and LDC. Based on the above discussions, we define *Relative Reliability Factor (RRF)* as the probability that for a particular channel occurrence H, the error rate of HDC is less than or equal to the error rate of LDC, i.e.:

$$RRF \overset{\Delta}{=} Prob\left(SER_{HDC} \leq SER_{LDC} \mid H\right) \qquad (52)$$

RRF is calculated for the channel (a) and the result is shown in Fig. 16. In this figure, the parameters are $m=2$, $M=3$, $L_{eq}=5$ and $D=5$. We observe that for $SNR \geq 25\, dB$, in almost 100 percent of the times, the performance of HDC is equal to or better than LDC. Also as observed from this figure, for $SNR=20\, dB$, although the average BER of HDC is worse than LDC (Fig. 5), we can still trust the system in almost 98 percent of the channel realizations. We conclude that at moderate and higher SNRs, HDC technique offers a high relative reliability.

VI. COMPARISON OF HDC AND LDC COMPLEXITIES

In this section we compare the complexity of HDC and LDC techniques and show that HDC has a considerably less complexity.

A. Memory Usage

HDC is a memoryless system. This property provides many benefits, like low cost, low power consumption and low hardware complexity. On the other hand, LDC technique requires $2M \times (L_{eq}-1)$ memories. Especially, for long impulse response channels (high values of L_{eq}) and high values of M, the number of required memories is significant, and therefore the cost and the complexity of the system are increased.

B. Computational Complexity

The computational complexity of HDC and LDC techniques is proportional to the number of coefficients of their filters. To present a quantitative comparison for computational complexity, we define the *complexity ratio* as:

$$Cxr \overset{\Delta}{=} \frac{The\ number\ of\ taps\ in\ LDC}{The\ number\ of\ taps\ in\ HDC} \qquad (53)$$

If we assume that the number of diversity branches is the same for both techniques, we have from equations (22) and (29):

$$Cxr = \frac{2\,L_{eq}}{(D+1)} \qquad (54)$$

As an example, for $D=5$ and $L_{eq}=5,9,15$, the complexity ratio is $Crx=1.66,3,5$ respectively. This

means that the computational complexity of HDC is almost 1.66, 3, 5 times lower than LDC respectively. This is a significant advantage for HDC technique, especially for long impulse response channels.

C. Equipments

Another valuable advantage of HDC technique over LDC is that in this system, we need a lower number of diversity branches. As we can observe from Fig. 5, at higher SNRs the performance of HDC for a lower number of diversity branches M, is even better than LDC performance with a higher values of M. From this figure we observe that the performance of HDC for the channel (a) with $M = 3$, is better than the performance of LDC with $M = 4$ when $SNR \geq 27.5\ dB$. Also we observe that in this case the performance of HDC with $M = 2$ is better than the performance of LDC with $M = 4$ when $SNR \geq 37\ dB$.

Hence, we can save the number of diversity branches, by using HDC technique. Consequently the number of antennas (in spatial diversity), correlators and other equipments required in the receiver are decreased.

At the end of this section, we consider a demonstrative example. In Fig. 17, the results of our simulation for HDC with $M = 5$, $m = 4$ and $D = 5$ are compared with LDC with $M = 8$, $m = 2$ and $L_{eq} = 9$ for the channel (c). Conclusions obtained from this comparison are summarized in Table 1.

VII. CONCLUSION

In this paper we presented a nonlinear low complexity memoryless combining technique based on Hammerstein type filters. We employed m-arry PAM modulation and assumed frequency selective Rayleigh fading channels with different power delay profiles. The performance of our proposed system was evaluated for different number of diversity branches and polynomial orders. Comparison of our simulation results with the results that we obtained from linear combining technique, shows that:

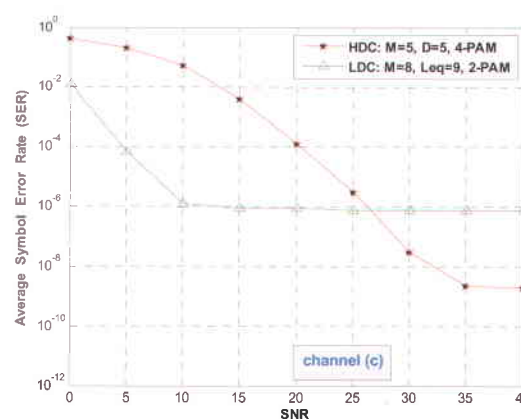a- At higher SNRs, the system performance of HDC is superior to LDC

Fig. 17. Average SER for HDC with $D = 5$ $M = 5$ and 4-PAM, and LDC with $L_{eq} = 9$ $M = 8$ and 2-PAM, for the channel (c)

b- At higher SNRs, in contrast to LDC, the system performance of HDC can be improved considerably by increasing the number of diversity branches

c- The superiority of HDC to LDC at higher SNRs, is valid for different power delay profiles

d- At moderate and high SNRs and for any channel occurrence, there is a high probability that the error rate of HDC is better than or equal to LDC

e- Analysis of the average minimum MSE performance of HDC system, verifies our simulation results

f- HDC provides a considerable low complexity technique as it needs less number of diversity branches, memories and computations than LDC

Table 1. Comparison of HDC with $D = 5$ and LDC with $L_{eq} = 9$ for the channel (c)

	Average BER	RRF (percent)	Number of Coefficients	Number of Diversity Branches	Number of Correlators	Memory Usage	Bandwidth Usage
HDC at SNR = 22 dB	2 e -5	98.23	30	5	10	0	W
HDC at SNR = 26 dB	7.22 e -7	99.81					
HDC at SNR = 35 dB	1.7 e -9	100					
LDC at SNR = 22 dB	8 e -7	-----	144	8	16	128	2 W
LDC at SNR = 26 dB	7.22 e -7	-----					
LDC at SNR = 35 dB	6.8 e -7	-----					

REFERENCES

[1] J. G. Proakis, and M.Salehi, Digital Communications, Fifth ed. New york: McGraw-Hill, 2008.

[2] M. K. Simon, and M. S. Alouini, Digital Communication Over Fading Channels, 2nd ed. New Jersey: John Wiley & Sons, 2005.

[3] H. C. Yang, and M. S. Alouini, "Improving the performance of switched diversity with post-examining selection," IEEE Trans. Wireless Communications., vol. 5, no. 1, pp. 67-71, Jan. 2006.

[4] R. You, H. Li, and Y. Bar-Ness, "Diversity combining with imperfect channel estimation," IEEE Trans. Communications., vol. 53, no. 10, pp. 1655-1662, Oct. 2005.

[5] R. K. Mallik, "Optimized diversity combining with imperfect channel estimation," IEEE Trans. Infor. Theory, vol. 52, no. 3, pp. 1176-1184, Mar. 2006.

[6] A. A. Basri, and T. J. Lim, "Optimum combining in rician / rayleigh fading environment with channel estimation errors," in Proc. IEEE Sym. Communications, Jun. 2006, vol. 1, pp. 274-278.

[7] J. Jeraj and V. J. Mathews, "A stable adaptive Hammerstein filter employing partial orthogonalization of the input signals," IEEE Trans. on Signal Processing, vol. 54, no. 4, pp. 1412-1420, 2006

[8] J. Jeraj and V. J. Mathews, "Stochastic mean-square performance analysis of an adaptive Hammerstein filter," IEEE Trans. on Signal Processing, vol. 54, no. 6, pp. 2168-2177, 2006.

[9] N. Kalouptsidis, and P. Koukoulas, "Blind identification of Volterra-Hammerstein systems," IEEE Trans. on Signal Processing, Vol. 53, Issue 8, Part 1, pp.2777 - 2787, Aug. 2005.

[10] F. Mkadem and S. Boumaiza, "Extended Hammerstein behavioral model using artificial neural networks," IEEE Trans. Microwave Theory and Techniques, vol. 57, no. 4, pp. 745-751, 2009.

[11] J. M. Le Caillec, "Time series modeling by a second-order Hammerstein system," IEEE Trans. on Signal Processing, vol. 56, no. 1, pp. 96-110, 2008.

[12] K. Shi, X. Ma and G. Tong Zhou, "Acoustic echo cancellation using a pseudocoherence function in the presence of memoryless nonlinearity," IEEE Trans.Circuits and Systems, vol. 55, no. 9, pp. 2639-2649, 2008.

[13] K. Shi, G. Tong Zhou and M. Viberg, "Compensation for nonlinearity in a Hammerstein system using the coherence function with application to nonlinear acoustic echo cancellation," IEEE Trans. on Signal Processing, vol. 55, no. 12, pp. 5853-5858, 2007.

[14] D. Zhou and V. DeBrunner, "Efficient adaptive nonlinear filters for nonlinear active noise control," IEEE Trans.Circuits and Systems, vol. 54, no. 3, pp. 669-681, 2007.

[15] X. N. Fernando, A. B. Sesay, "A Hammerstein type equalizer for the Wiener type fiber wireless channel," in Proc. IEEE Conf. PACRIM '01, Aug. 2001, vol. 1, pp. 546-549.

[16] X. N. Fernando and A. B. Sesay, "A Hammerstein type equalizer for concatenated fiber-wireless uplink," IEEE Trans. Vehicular Tech., vol. 54, no. 6, pp. 1980–1991, 2005.

[17] Y. Miar, and H. Amindavar, "Hammerstein decision feedback equalization (HDFE) as a new equalizer of GSM receivers," IEEE International Sym. Signal Processing and its Applications (ISSPA), Paris, France, July 2003.

[18] Y. Miar, A. R. Momen, H. AminDavar and H. Samimi, "Blind Hammerstein decision feedback equalizer (BHDFE) as a new blind equalizer," in proc. IEEE Canadian Conference on Electrical and Computer Engineering, Niagara Falls, Canada, May 2004, Vol. 1, pp. 567- 570.

[19] S. M. Kay, Fundamentals of Statistical Signal Processing, New Jersey: Prentice Hall, 1993.

[20] B. Glance and L. J. Greenstein, "Frequency-selective fading effects in digital mobile radio with diversity combining," IEEE Trans.Communications. vol. 31, no. 9, pp. 1085-1094, 1983.

[21] M. Wittmann, J. Marti and T. K¨urner, "Impact of the power delay profile shape on the bit error rate in mobile radio systems," IEEE Trans. Vehicular Tech., vol. 46, no. 2, pp. 329-339, 1997.

Amir Masoud Aminian Modarres received the B.S. degree in electronic engineering and the M.S. and Ph.D. degrees in communication engineering from Ferdowsi University of Mashhad, Iran, in 1995 and 2002 and 2009, respectively. Since 2002 he has been a faculty member in department of electrical engineering at Sadjad Institute of Higher Education, Mashhad, Iran. His current interests are digital communications, signal processing and cryptography.

Dr. Mohammad Molavi Kakhki (S. M. IEEE 1993) received the B.S. degree in physical electronics in 1971 from university of Tabriz, Iran, and M.S. and Ph.D. degrees in electronic communications from University of Kent at Canterbury, UK. in 1977 and 1981 respectively. From 1981 to 1984 he worked as a research fellow at Kent University. In 1985 he joined department of electrical engineering at Ferdowsi University of Mashhad, Iran, and he is currently an associate professor in this university. His current interests are optical communications, digital communications and power line communications.